

# Crystallization of poly(vinylidene fluoride) during ultra-fast cooling

A. Gradys<sup>a,\*</sup>, P. Sajkiewicz<sup>a</sup>, S. Adamovsky<sup>b</sup>, A. Minakov<sup>b,c</sup>, C. Schick<sup>b</sup>

<sup>a</sup> Institute of Fundamental Technological Research, Polish Academy of Sciences, Swietokrzyska 21 00-049 Warsaw, Poland

<sup>b</sup> Universitaet Rostock, Institut für Physik Universitaetsplatz 3, 18051 Rostock, Germany

<sup>c</sup> A.M. Prokhorov General Physics Institute, Vavilov 38, 119991 Moscow, Russia

Available online 3 June 2007

## Abstract

Melt-crystallization of polyvinylidene fluoride (PVDF) was investigated in non-isothermal mode at ultra-high cooling rates ranging between 30–3000 K/s as well as at constant temperatures after quenching at 6000 K/s. An increase of the cooling rate above 150 K/s leads to the formation of  $\beta$  phase manifested by a low temperature shoulder of crystallization exotherm in addition to the  $\alpha$  modification. At the cooling rates above 2000 K/s there is only low temperature exothermic peak that is attributed to the crystallization of pure  $\beta$  modification. Isothermal crystallization was possible to realize at 110 °C as the lowest, resulting in  $\alpha$  form. Much higher crystallization rate in submicrogram samples, as compared to standard DSC experiments, is also reported.

© 2007 Elsevier B.V. All rights reserved.

**Keywords:** Polyvinylidene fluoride; Crystallization; Ultra-fast calorimetry; Polymorphism

## 1. Introduction

Poly(vinylidene fluoride) is known to exist in several crystal modifications. Upon cooling from melt at conventional rates the non-polar  $\alpha$  form is obtained. When the crystallization is conducted at much lower cooling rates and/or at temperatures above ca. 155 °C an additional  $\gamma$  form appears [1,2].

The solid state transition of  $\alpha$  modification may be obtained at high and very high electrostatic field, resulting in formation of  $\delta$  and  $\beta$  phase, respectively [3]. The  $\beta$  modification can be also obtained directly from melt under the influence of electrostatic field [4]. As is reported in [5] from structural studies of final states, application of very high cooling rates as ca. 800 K/s, leads to melt-crystallization of  $\beta$  PVDF.

Our work was focused on the calorimetric investigations of melt-crystallization of PVDF during ultra-fast cooling up to 3000 K/s as well as at constant temperature approached by quenching at 6000 K/s. The aim of the work was to analyze transitions occurring at those conditions, where occurrence of the  $\beta$  modification might be expected.

## 2. Experimental

Poly(vinylidene fluoride) (PVDF) Kynar 880N (Pennwalt Corp.) with  $M_w = 400 \times 10^3$ ,  $M_n = 149 \times 10^3$ , and a content of head-to-head defects of 5.2% was investigated.

The experiments were mainly conducted using thin-film chip calorimeter based on a thermal conductivity gauge TCG-3880, Xensor Integrations [6]. The cell consists of a submicron  $\text{Si}_3\text{N}_x$  membrane with a resistive film-heater and a film-thermopile located at the center of the membrane. The current to the heater as well as voltage from the thermopile are measured simultaneously. The temperature dependencies of the heater resistance as well as the thermopile sensitivity were determined in advance. Determination of the temperature dependence of the coefficient of heat exchange between the heating region and environment which enables to calculate heat capacity of the sample as well as full description of the sensor control can be found in [7,8]. The experiments were conducted using the system consisting of the sensor mounted inside a vacuum shielded oven. The whole construction is designed to fit into a Dewar vessel with liquid nitrogen. A Cu-Constantan thermocouple located close to the sensor enables measuring surrounding gas temperature. Thus stable temperature and pressure conditions for the holder were provided. More complete description of the system might be found elsewhere [8,9]. The experiments on all samples were performed at holder temperature  $-100$  °C and nitrogen pressure of

\* Corresponding author. Tel.: +48 22 8261281x211; fax: +48 22 8269815.  
E-mail address: [argrad@ippt.gov.pl](mailto:argrad@ippt.gov.pl) (A. Gradys).

10 kPa. The weight of sample used for measurements was calculated from specific heat capacity in the molten state provided by ATHAS databank [10] and was found to be ca. 460 ng.

Prior to crystallization the sample was kept at molten state at 245 °C for 0.01 s. Application of such extremely short time of melting is forced by specific technical requirements of the chip calorimeter. Relatively high temperature of melting is believed to compensate short time. Application of those conditions is assumed to erase the thermal history and to avoid the degradation, enabling thus the processing of the sample for many cycles. The experiments in the non-isothermal mode consisted of cooling and heating scans between 245 and –100 °C at rates in the range of 30–3000 K/s. The isothermal experiments were performed at various temperatures ranging from 60 to 180 °C at holding time of 5 s. The sample was quenched from the melt to the isothermal temperature at 6000 K/s at the maximum. Supplementary information on the crystallization process was drawn from subsequent heating scans at 1100 K/s.

For comparison experiments on standard DSC apparatus Perkin-Elmer Pyris-1 were also performed. Before cooling, standard melting procedure was applied, i.e. samples weighing few mg were kept at 220 °C for 10 min.

### 3. Results and discussion

#### 3.1. Non-isothermal crystallization.

Cooling scans performed at various rates showing changes in the heat capacity of a PVDF sample are presented in Fig. 1.

It is seen in Fig. 1 that at cooling rates below 150 K/s there is only one crystallization peak, shifting to lower temperatures with increasing cooling rate. At the rates between 150 and 1500 K/s an additional low temperature shoulder appears, which at the rates higher than 2000 K/s may be seen as the only low temperature crystallization peak. From the literature, it may be supposed that the high temperature peak pertains to crystallization of the

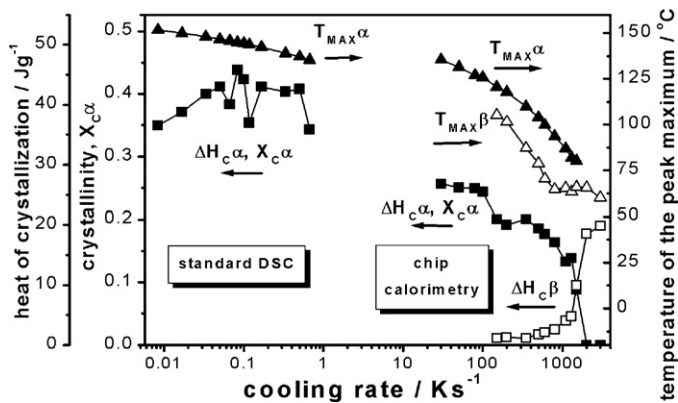


Fig. 2. Heat of crystallization,  $\Delta H_C$ , and the temperature of peak maximum,  $T_{MAX}$ , of  $\alpha$  and  $\beta$  peaks as a function of cooling rate. Crystallinity of  $\alpha$  phase determined with the enthalpy of melting  $\Delta H^0_{\alpha} = 104.5 \text{ J/g}$  [10]. DSC results obtained on samples weighing ca. 7 mg.

$\alpha$  form, while the low temperature peak may be ascribed to crystallization of the  $\beta$  form [5]. To the knowledge of the authors, it is for the first time that the direct evolution of the crystallization heat of  $\beta$  form in PVDF is reported. Our results indicate that at the highest cooling rates ranging between 2000 and 3000 K/s, crystallization of  $\alpha$  form is stopped resulting in formation of  $\beta$  phase, only (Fig. 2). Moreover, it is seen in Fig. 1 that glass transition observed at high cooling rates occurs at higher temperature (ca. –45 °C) than the value reported in ATHAS databank (–61 °C) [10].

Fig. 2 shows the heat of crystallization and the temperature of peak maximum of  $\alpha$  and  $\beta$  forms as a function of cooling rate. First, it is seen inconsistency of the dependence of the position of  $\alpha$  crystallization peak for both techniques which will be discussed further. In the case of  $\alpha$  modification, the knowledge of the enthalpy of melting,  $\Delta H^0_{\alpha}$  [10], allows determination of crystallinity as a function of cooling rate. The lack of literature data of melting enthalpy of  $\beta$  form, makes the determination of  $\beta$  crystallinity impossible. The method that could be helpful in determination of the phase content is the analysis of the change in the heat capacity at the glass transition temperature ( $\Delta C_p$  at  $T_g$ ). By this method, one could determine the content of amorphous phase, provided the knowledge of theoretical  $\Delta C_p$ . Then, assumption of two phases, i.e. mobile amorphous and crystalline, allows determination of crystallinity. We expected that in the case of fast cooled PVDF, containing  $\beta$  form, it allows us determination of  $\beta$  crystallinity. The examples of the heating scans at 100 and 2000 K/s recorded subsequently after cooling scans in the range 100–2000 K/s are presented in Fig. 3a and Fig. 3b, respectively. It was found, that the changes in the heat capacity,  $\Delta C_p$ , registered at  $T_g$  during subsequent heating were practically independent of the applied cooling rate (see insights in Fig. 3a and Fig. 3b); the same behavior was observed for all heating rates in range 100–2000 K/s. One reason of this observation may be that reasonably small changes in the total crystallization heat ( $\Delta H_{C\alpha} + \Delta H_{C\beta}$ , Fig. 2), related to the final crystallinity are probably below sensitivity to be reflected by the corresponding change in the  $\Delta C_p$  at  $T_g$  during subsequent heating.

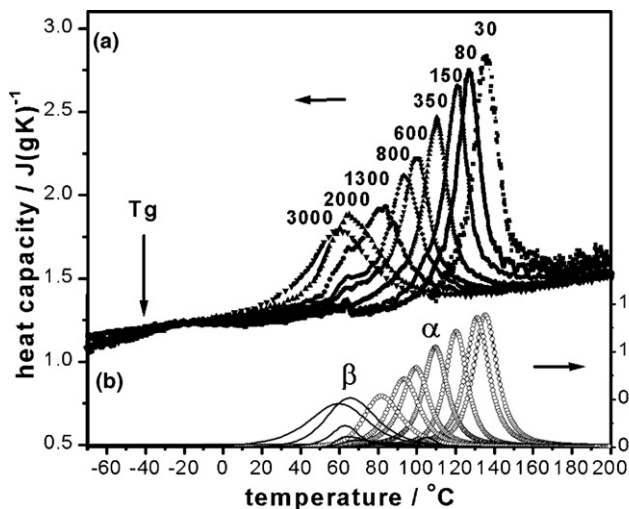


Fig. 1. Thermograms (a) as registered and (b) after deconvolution using Pearson VII function into  $\alpha$  and  $\beta$  peaks, during cooling at various rates (indicated in K/s).

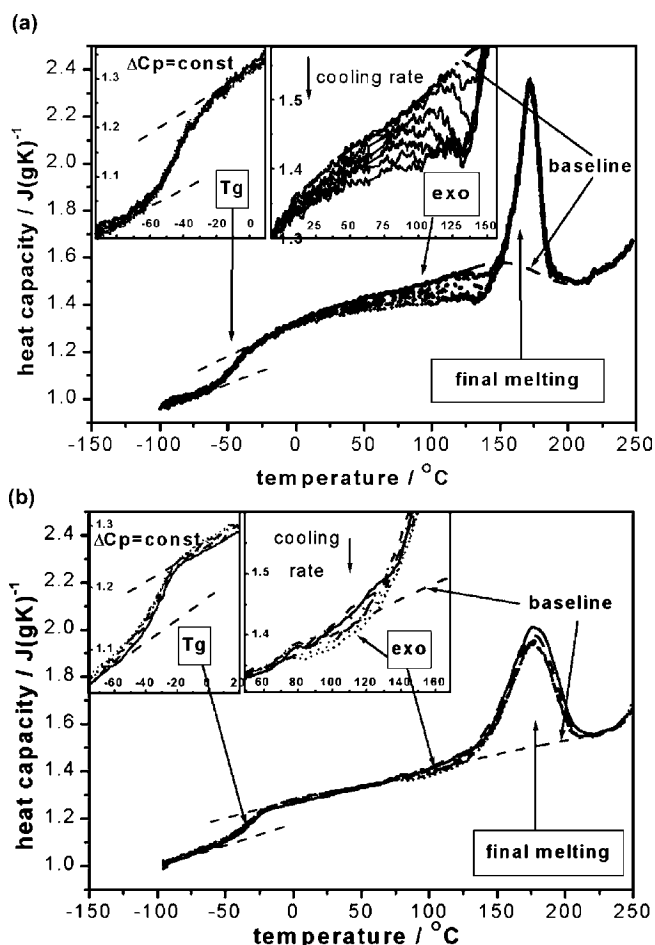


Fig. 3. Thermograms registered during heating at (a) 100 K/s and (b) 2000 K/s, after cooling at the rates between 100 and 2000 K/s.

Another explanation needs consideration of the three-phase model and appearance of the rigid amorphous phase. Though, as measured at the same heating rate, the cooling rate seems not to affect  $\Delta C_p$  at  $T_g$ , we measured different values of  $\Delta C_p$  at  $T_g$ , while changing the heating rate. At the lowest heating rate applied 100 K/s (Fig. 3a), the  $\Delta C_p$  at  $T_g$  was the highest ca. 0.14 J/(gK), what corresponds to ca. 0.4 of the mobile amorphous fraction, assuming  $\Delta C_p$  at  $T_g$  for 100% of amorphous fraction as 0.331 J/(gK) [10]. There may be a large uncertainty related with determination of the mobile amorphous phase content, but assuming the 0.4 value and regarding that the  $\alpha$  crystallinity obtained at cooling of 100 K/s is ca. 0.25, it seems that the intermediate rigid amorphous phase, which is not involved in the glass transition, should be around 0.35. Then, the expected decrease in crystallinity with increasing cooling rate and no change in  $\Delta C_p$  at  $T_g$  could be justified by an increase in the rigid amorphous phase content.

Moreover, the heating scans in Fig. 3 indicate the occurrence of relatively complex changes at temperatures above the glass transition temperature. In addition to the large endothermic peak, related to the final melting, there is an exothermic effect occurring in the temperature range between the glass transition and the melting. An increase in the cooling rate leads to an increasing in area of the exothermic peak. At the same time, this

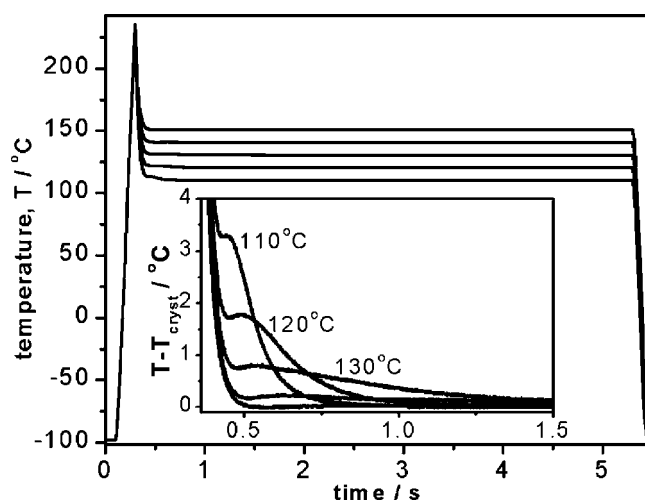


Fig. 4. Temperature profiles,  $T$ , as registered during isothermal experiments. The inset shows crystallization peaks after subtraction of the respective isothermal crystallization temperature,  $T_{\text{cryst}}$  (indicated), determined as the constant after the crystallization peak.

exothermic effect is suppressed by increasing the heating rate. The exothermic effect, observed for both samples crystallized in pure  $\alpha$  as well as in  $\beta$  form, may be related to reorganization or polymorphic transitions from the states being very far from equilibrium.

### 3.2. Isothermal crystallization

Examples of the temperature profiles registered during isothermal processes are presented in Fig. 4. One observes the temperature peaks due to release of the crystallization heat. The inset in Fig. 4 shows comparison of the crystallization peaks registered at various temperatures, shown as the temperature difference between registered and isothermal crystallization temperature determined after the crystallization peak,  $T - T_{\text{cryst}}$ .

Quenching of the sample caused exponential approach to the desired isothermal crystallization temperature,  $T_{\text{cryst}}$ . Double exponential decay function was used for fitting of the temperature profile during quenching,  $T_{\text{fit}}$  (Fig. 5). Result of subtraction of the best fit from the registered temperature profile,  $T - T_{\text{fit}}$  (the inset in Fig. 5), showed non-zero value of  $T - T_{\text{fit}}$  preceding the crystallization peak, making determination of the peak starting time,  $t_0$ , difficult. The  $t_0$  was chosen as the local minimum preceding the crystallization peak. This enabled determination of the time of the temperature peak maximum,  $t_p$ , with respect to the starting time,  $t_0$ , (inset in Fig. 5). The lowest successful isothermal crystallization temperature was 110°C; below that temperature crystallization occurred mainly upon quenching.

Isothermal processes performed above 150°C led to very low crystallization heat flow rate making further analysis in this way difficult. However, additional information on the isothermal crystallization could be obtained from the analysis of heating scans, registered subsequently after isothermal processes. Fig. 6 shows the melting behavior of isothermally crystallized sample. It was difficult to determine the onset of the melting peaks, thus only positions of the peaks maximum were given,  $T_m$ .

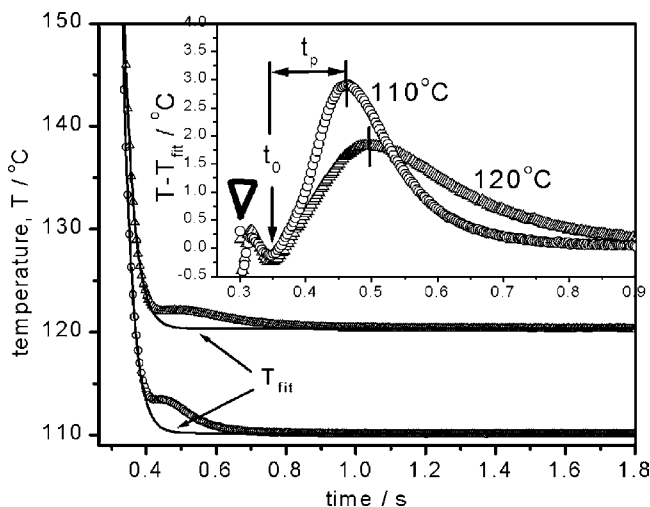


Fig. 5. Example temperature profiles,  $T$ , as registered (points), and the best double exponential decay fits of the quenching (solid lines)  $T_{\text{fit}}$ . The inset shows the result of subtraction of the registered temperature,  $T$ , and  $T_{\text{fit}}$ , for two crystallization temperatures (indicated), which helps determine the starting time  $t_0$  and the maximum  $t_p$  of the crystallization peak. Triangle indicates the start of the cooling from melt.

The crystallization temperature dependencies of the kinetic parameter,  $t_p$ , and of melting behavior,  $T_m$  and  $\Delta H$ , are collected in Fig. 7a and Fig. 7b, respectively. For comparison, results for  $\alpha$  phase crystallization obtained with standard DSC were added. It seems rather clear that the chip calorimetry isothermal crystallization data relate to  $\alpha$  phase, only. As revealed by non-isothermal experiments (see the previous section) crystallization of  $\beta$  form should be expected below  $100^\circ\text{C}$ , which is much lower than approached isothermally. The structure of the phase obtained at the highest temperatures may be questionable. As it was mentioned in the introduction above  $155^\circ\text{C}$ , the  $\gamma$  phase appearance is reported [1,2]; however, uninflected  $T_m$  temperature dependence gives no evidence of this behavior (Fig. 7b).

It is seen in Fig. 7 that with decrease of the temperature of isothermal crystallization, the crystallization rate increases, which is manifested by a reduction of the time  $t_p$ . It indicates

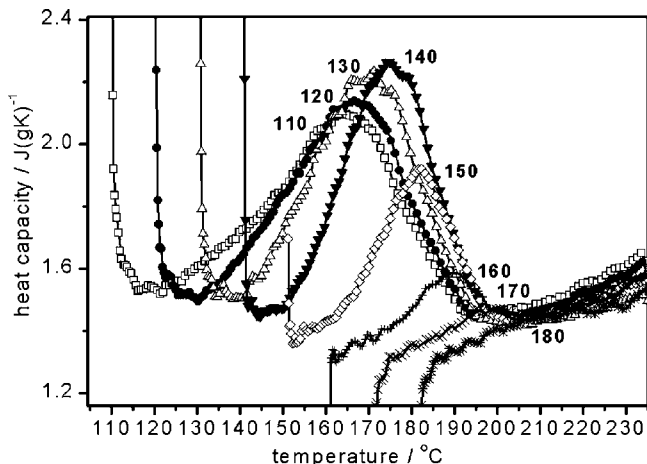


Fig. 6. Heating scans at 1100 K/s recorded subsequently after isothermal steps for 5 s at temperatures indicated in  $^\circ\text{C}$ .

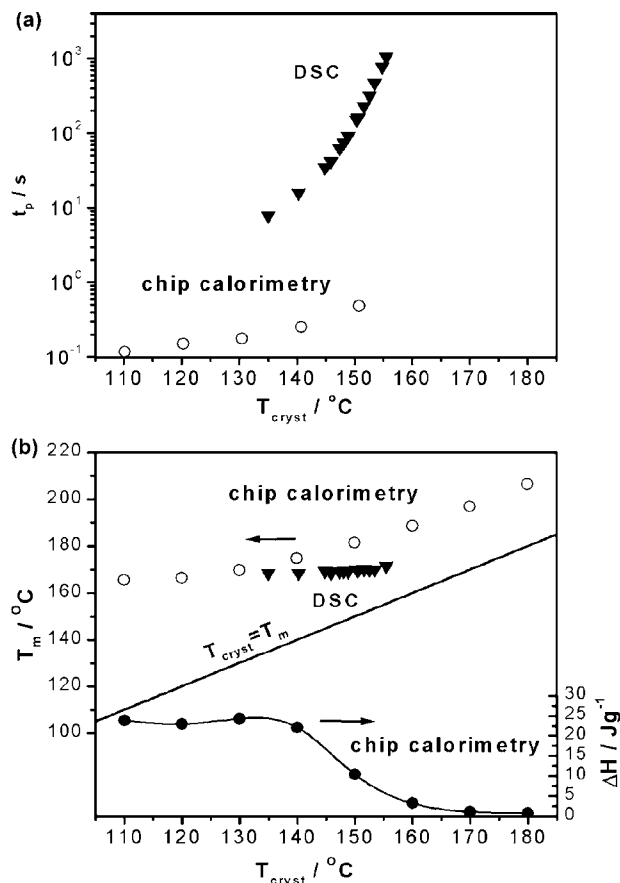


Fig. 7. Crystallization temperature,  $T_{\text{cryst}}$ , dependencies of (a) the time of the crystallization peak maximum,  $t_p$ , (b) the temperature of maximum of the melting peak,  $T_m$  and the heat of melting,  $\Delta H$ . Open and solid circles: chip calorimetry, solid triangles: standard DSC results for  $\alpha$  phase. In case of DSC experiments,  $t_p$  was determined as the maximum of the heat flow rate peak and  $T_m$  from the heating scans at 40 K/min (0.67 K/s), on samples weighing ca. 2 mg (not shown). Note that  $T_m$ , as obtained from the chip calorimetry (Fig. 7b), is affected by superheating at 1100 K/s [11].

that the maximum rate of  $\alpha$  crystallization is below  $110^\circ\text{C}$ . One should also expect a decrease in the induction time connected with formation of stable nuclei, which has been observed in case of DSC experiments. However, from the analysis of the heating scans (Fig. 6), it may be understood that, in case of the chip calorimetry experiments, in spite of short holding time (5 s), the melting peak is still to be found even up to  $T_{\text{cryst}} = 180^\circ\text{C}$  (Fig. 7b). Decreasing area of the melting peak  $\Delta H$  (Fig. 7b, below), starting from crystallization temperature of  $140^\circ\text{C}$  and above, indicates 5 s being not sufficient to complete crystallization.

The data shown in Fig. 7a provide additional evidence of the large discrepancy in the crystallization kinetics derived from both instruments. It is seen that for instance at  $140^\circ\text{C}$ ,  $t_p$  is a two orders shorter in the case of chip calorimetry than for standard DSC. Regarding our observation that crystallization is much faster in the case of chip calorimetry than for standard DSC, there are few possible reasons. The first one is related to different melting conditions applied by us in both instruments. In case of the chip calorimetry the time applied for melting should be very short (0.01 s in our experiments). Although the

temperature of melting was relatively high (240 °C) we can not exclude that the applied conditions were insufficient to attain the equilibrium melt, and subsequent crystallization may be much faster because of the local order present in the melt. Additional experiments with various melting temperatures (between 220 and 250 °C) and still the same time of melting (0.01 s) showed that the temperature of the crystallization peak during subsequent cooling was independent of the melting temperature. The only effect was the reduction of area of crystallization peak after melting at temperatures below 235 °C. One of the possible interpretations is that the melting conditions applied are not sufficient to allow segmental diffusion and thus attainment of the equilibrium melt, making nucleation much easier. The reduction of crystallization peak indicates that after melting below 235 °C there is a remaining macroscopic fraction of unmelted crystallites.

Another explanation of much faster crystallization observed in the case of chip calorimetry may come from the enhanced nucleation at the chip-membrane/polymer interface.

#### 4. Conclusions

Our results indicate that it is possible to obtain pure  $\beta$  phase in PVDF during crystallization from the melt at cooling rates above ca. 2000 K/s. Since the structure obtained at ultra-high cooling rates is very far from equilibrium, it is very difficult to interpret transitions registered during subsequent heating using calorimetry, only. The exothermic peak observed during heating at temperatures below melting is interpreted by us as a transition of a very unstable structure towards an equilibrium state. From the analysis of crystallization heat during cooling and the change of specific heat at glass transition it is quite probable that in addition to crystal and amorphous phase, so-called rigid amorphous phase should be considered. The amount of rigid amorphous phase seems to increase with rate of cooling. Addi-

tional advantage of ultra-fast calorimetry is the possibility to perform isothermal crystallization at temperatures, which are not accessible using standard calorimetry. This is realized by very fast cooling before the isothermal step. Surprisingly, isothermal crystallization processes could not be performed lower than 110 °C, due to high rate of crystallization. Our results indicate that the maximum rate of  $\alpha$  crystallization occurs below 110 °C. The reasons for much faster crystallization as registered with chip calorimetry as compared to standard DSC are not clear at the moment and need further investigation.

#### Acknowledgement

The investigations using ultra-fast calorimeter were performed at the University in Rostock in the frame of COST Action P12 “Structuring of Polymers” as the Short Term Scientific Mission COST-STSM-P12-00656.

#### References

- [1] P. Sajkiewicz, *Eur. Polym. J.* 35 (1999) 1581–1590.
- [2] R. Gregorio Jr., R.C. Capita, *J. Mater. Sci.* 35 (2000) 299–306.
- [3] D. Naegel, D.Y. Yoon, *Appl. Phys. Lett.* 33 (1978) 132–134.
- [4] S.L. Hsu, F.J. Lu, D.A. Waldman, M. Muthukumar, *Macromolecules* 18 (1985) 2583–2587.
- [5] Y. Oka, N. Koizumi, *Bull. Inst. Chem. Res., Kyoto Univ.* 63 (1985) 192–206.
- [6] A.W. van Herwaarden, *Thermochim. Acta*, 432 (2005) 192, <http://www.xensor.nl/txtfiles/hfdfiles/prodstan.htm>.
- [7] S.A. Adamovsky, A.A. Minakov, C. Schick, *Thermochim. Acta* 403 (2003) 55–63.
- [8] A.A. Minakov, S.A. Adamovsky, C. Schick, *Thermochim. Acta* 432 (2005) 177.
- [9] S. Adamovsky, C. Schick, *Thermochim. Acta* 415 (2004) 1–7.
- [10] ATHAS Data Bank M. Pyda (Ed), web address: <http://athas.prz.edu.pl/databank/intro.html>.
- [11] A.A. Minakov, A.W. van Herwaarden, W. Wien, A. Wurm, C. Schick, *Thermochim. Acta*, in press.